FSAR 1978
Food Science of Animal Resources
Food Sci. Anim. Resour. 2024 January 44(1):204~215
DOI https://doi.org/10.5851/kosfa.2023.e74
pISSN : 2636-0772 eISSN : 2636-0780
http://www.kosfaj.org

ARTICLE

Oral Administration of *Lactilactobacillus curvatus* LB-P9 Promotes Hair Regeneration in Mice

Mikyung Song, Jaeseok Shim, and Kyoungsub Song*
R&D Center, LISCure Biosciences Inc., Seongnam 13486, Korea

OPEN ACCESS

Received October 25, 2023
Revised November 3, 2023
Accepted November 13, 2023

*Corresponding author : Kyoungsub Song
R&D Center, LISCure Biosciences Inc.,
Seongnam 13486, Korea
Tel: +82-31-706-1712
Fax: +82-31-706-1718
E-mail: kssong@liscure.bio

*ORCID
Mikyung Song
https://orcid.org/0009-0001-8279-0338
Jaeseok Shim
https://orcid.org/0009-0003-3228-7448
Kyoungsub Song
https://orcid.org/0009-0005-3395-3689

Abstract This study was designed to examine the effect of *Lactilactobacillus curvatus* LB-P9 on hair regeneration. The treatment of LB-P9 conditioned medium increased the proliferation of both hair follicle dermal papilla cells and hair germinal matrix cells (hGMCs). Moreover, the expression levels of hair growth factors such as vascular endothelial growth factor (VEGF) and fibroblast growth factor 7 were significantly elevated in hGMCs co-cultured with LB-P9. After time-synchronized depilation, mice were orally administered with either 4×10^7 colony forming unit (CFU) of LB-P9 (low dose) or 4×10^8 CFU of LB-P9 (high dose), once daily for 4 weeks. Compared with the vehicle (phosphate-buffered saline)-administrated group, the LB-P9-treated groups exhibited accelerated hair regrowth rate and enhanced hair thickness in a dose-dependent manner. Supporting this observation, both hair follicle numbers and the dermal thickness in skin tissues of the LB-P9-treated groups were increased, compared to those of the vehicle-treated group. These results might be explained by the increased level of β-catenin and number of hair follicle stem cells ($CD34^+CD49f^+$ cells) in the skin tissues of mice administered with LB-P9, compared to the vehicle-treated mice. Also, increased serum levels of hair growth factors such as VEGF and insulin-like growth factor-1, and superoxide dismutase were found in the LB-P9-treated groups, compared to those of the vehicle-treated group. Taken together, these results might demonstrate that the oral administration of LB-P9 promotes hair regeneration by the enhancement of dermal papilla proliferation through the stimulation of hair growth factor production.

Keywords hair growth factor, hair regeneration, probiotics

Introduction

Hair loss is a common disorder that occurs in both men and women (Tamashunas and Bergfeld, 2021). This has resulted in increased interest in health and beauty, with particular emphasis on hair as a significant factor in assessing one's appearance and attractiveness (Tamashunas and Bergfeld, 2021). At present, several chemical drugs, such as minoxidil and finasteride, are widely used for the prevention of further hair loss (Bajoria et al., 2023). However, several recent clinical studies have indicated that the clinical effectiveness of minoxidil or finasteride has remained low, with response rates of 35% or 48%, respectively (Bajoria et al., 2023). Also, unwanted side effects that

include irritation, itchiness, and abnormal sexual function have been reported (Nestor et al., 2021). These limitations have encouraged the development of alternative treatment strategies.

Many studies now focus on developing specific probiotics products for use as a major tool to change human physiology related to well-being in life. The communication between host mucosal barrier cells and selective probiotics might create new signals that change important physiological parameters within specific tissues or organs after reach (Belkaid and Hand, 2014). These physiological changes by the consumption of particular probiotics were further explained by the results from the gut-specific organ axis (Dumas et al., 2018; Powell et al., 2017; Tripathi et al., 2018). In particular, recent findings in the gut-brain-skin axis have demonstrated that probiotics both control skin inflammation, and regulate hair follicle cycling or hair regeneration (Arck et al., 2010). Indeed, several previous experiments reported that the administration of particular probiotics might enhance hair growth (Lee et al., 2016; Nam et al., 2021; Park et al., 2020).

In the present study, we examined the effect of *Lactilactobacillus curvatus* LB-P9 on hair regeneration. Both the *in vitro* and *in vivo* data suggest that LB-P9 administration might promote hair regeneration by facilitating dermal papilla growth via the enhancement of hair growth factor production. The results of this study may provide additional evidence to define the molecular mechanisms of how the consumption of probiotics enhances hair growth.

Materials and Methods

Probiotics

L. curvatus LB-P9, originally isolated from Kimchi, was obtained from the World Institute of Kimchi (Gwangju, Korea) via a technology transfer agreement. Species level of LB-P9 was identified by the alignment of the obtained 16S rRNA sequence with the Genbank database (http://www.ncbi.nlm.nih.gov/BLAST). The stock of LB-P9 was deposited with accession number KCCM12011P at Korean Culture Center of Microorganisms (KCCM, Seoul, Korea). LB-P9 was kept as frozen stock in MRS broth (BD Difco, Sparks, MD, USA) containing 30% (v/v) glycerol at −80°C, until use. To thaw the frozen stock, LB-P9 was incubated in MRS broth at 30°C for 24 h, and then harvested by centrifugation (685×g, 20 min). The cell pellets were washed, and resuspended in sterile phosphate-buffered saline (PBS) for *in vitro* assays and animal studies.

Human hair cell culture

Human hair follicle dermal papilla cells (hFDPCs) were purchased from PromoCell (Heidelberg, Germany). The hFDPCs were cultured in FDPC growth medium supplemented with 4% (v/v) fetal calf serum, 0.4% (v/v) bovine pituitary extract, human recombinant basic fibroblast growth factor (1 ng/mL), and human recombinant insulin (5 μg/mL; PromoCell). Human hair germinal matrix cells (hGMCs) were obtained from ScienCell Research Laboratories (Carlsbad, CA, USA). The hGMCs were cultured in mesenchymal stem cell medium supplemented with 5% (v/v) fetal bovine serum, and 1% (v/v) mesenchymal stem cell growth supplement (ScienCell Research Laboratories). Both hFDPCs and hGMCs were cultured at 37°C in a humidified atmosphere of 5 % CO_2.

Measurement of hair cell proliferation after the treatment of LB-P9 conditioned medium

The 1×10^9 colony forming unit (CFU)/mL of LB-P9 was incubated with 50 mL of serum-free hFDPC culture medium (PromoCell) for 24 h at 30°C. After culture, LB-P9 conditioned medium (CM; pH=7.2) was collected from the culture supernatants by centrifugation at 685×g for 10 min, filtered through a Millipore membrane filter (pore size=0.22 μm), and

stored at −80°C, until use.

Both hFDPCs (1×10^4 cells/well) and hGMCs (1×10^4 cells/well) were plated into a 96-well plate in culture medium. After 24 h, LB-P9 CM was added at concentration of 0.25% or 0.5%, adjusted the final culture volume in 200 μL/well and cultured for an additional 24 h. After culture, cell proliferation was evaluated using the WST-8 cell viability assay kit (Biomax, Guri, Korea), according to the manufacturer's protocol.

Quantitative reverse-transcriptase real-time polymerase chain reaction analyses

The hGMCs (2×10^5 cells/well) were plated into a 6-well plate in culture medium. After 24 h, LB-P9 (2×10^6 CFU/well) was added into each well, and cultured for additional 24 h. After culture, the total RNA from each sample was extracted using TRIZOL reagent (Thermo Fisher Scientific, Waltham, MA, USA) according to the manufacturer's protocol, and quantified using NanoDrop 2000 (Thermo Fisher Scientific). Each total RNA sample was then converted into cDNA using a cDNA synthesis kit (Thermo Fisher Scientific) according to the manufacturer's protocol.

Quantitative real-time polymerase chain reaction (PCR) was then carried out using 1 μg of each total RNA with SYBR Green real-time PCR master mix (Thermo Fisher Scientific) on a QuantStudio™ Real-Time PCR System (Thermo Fisher Scientific). The PCR was programmed with an initial denaturation at 95°C for 3 min, followed by 40 cycles at 95°C for 15 s, 60°C for 30 s, and 72°C for 30 s. The primer sequences for human *Vegf* were 5′-GAGGGCAGAATCATCACGAA-3′ (sense) and 5′-CACCAGGGTCTCGATTGGAT-3′ (anti-sense), resulting in an 80 bp product, while the primer sequences for human *Fgf7* were 5′-CTGTCGAACACAGTGGTACCTG-3′ (Forward) and 5′-CCAACTGCCACTGTCCTGATTTC-3′ (Reverse), resulting in a 108 bp product. To obtain relative gene expression, the expression levels of all the genes were normalized to those of the human *Gapdh*. The primer sequences for human *Gapdh* were 5′-GTCGGAGTCAACGGA TTTGG-3′ (sense) and 5′GGGTGGAATCAATTGGAACA-3′ (anti-sense), resulting in a 208 bp product.

Administration of LB-P9 in a hair regeneration animal model

Five-week-old male C57BL/6 mice were obtained from Doo Yeol Biotech (Seoul, Korea). Mice were acclimatized under constant conditions for one week. After acclimatization, the mice were anesthetized with isoflurane, and the back of each mouse was shaved using an animal clipper. After applying the depilatory agent, the remaining fine hairs on the skin were removed. After 24 h of skin stabilization, eighteen of the C57BL/6 mice with telogen phase hair were randomly divided into three groups (n=6 per group). One group of mice received the vehicle (200 μL of PBS) every day for 4 weeks, the second group of mice received a low dose of LB-P9 (4×10^7 CFU in 200 μL of PBS) every day for 4 weeks, and the third group of mice received a high dose of LB-P9 (4×10^8 CFU in 200 μL of PBS) every day for 4 weeks. Four weeks later, all the experimental mice were sacrificed for analyses. Mice were fed a standard diet with purified water *ad libitum*, and maintained at 22±3°C, 50±20% humidity, 150–300 lx, and 12 h/12 h light-dark cycle. All animal studies were conducted by CentralBio (Incheon, Korea), while the procedures of animal study were approved by the Institutional Animal Care and Use Committee of CentralBio (protocol number: CBIACUC 22-0478EF).

Visual analyses of hair regeneration

To visualize hair regeneration in the animal model, dorsal skin images were taken from each experimental mouse using a distal camera (Nikon, Tokyo, Japan) every 2 to 3 days starting at the initial feeding of LB-P9 until mice were sacrificed.

Digital images were analyzed using Image J software (National Institutes of Health, Bethesda, MD, USA) to calculate the hair growth rate (regrown area/total shaved area) in each mouse.

Measurement of thickness and surface structure of hairs

To analyze the hair thickness and hair cuticle shape, images of hairs obtained from randomly selected mice from each different treatment group were taken by scanning electron microscopy (HITACHI S-4700, Hitachi, Tokyo, Japan) at various resolutions. Digital images were analyzed using Image J software (National Institutes of Health) to measure the diameter of each hair, and visualize the morphology of cuticles on each hair.

Histological analyses of dorsal skin tissues

Each dorsal skin tissue sample was fixed in 4% neutral formalin, and embedded in paraffin blocks using a HistoStar™ embedding workstation (Thermo Fisher Scientific). Hematoxylin and eosin (H&E) staining was then performed with each tissue section (5 μm thickness) using a Dako CoverStainer (Agilent, Santa Clara, CA, USA). After staining, images of each H&E staining sample were taken under Zeiss Axiovert 200M microscopy (Carl Zeiss AG, Thornwood, NY, USA) at 100× magnification. Each image was then analyzed using Image J software (National Institutes of Health) to measure dorsal skin thickness and the number of hair follicles per unit area ($\times 10^4/\mu m^2$).

Western blot analyses

Each skin sample was homogenized with a RIPA buffer [50 mM Tris (pH 8.0), 150 mM NaCl, 0.5% sodium deoxycholate, 1.0% IGEPAL CA-630, 0.1% sodium dodecyl sulfate] containing protease inhibitor cocktail (Sigma-Aldrich, St. Louis, MO, USA). Proteins were extracted by centrifugation of each tissue homogenate at 4℃ and 21,206×g for 15 min, and quantified using the BCA protein assay kit (Pierce, Rockford, IL, USA). Each Protein sample was then denatured by heating at 95℃ for 5 min, separated by electrophoresis on Bolt™ Bis-Tris Plus Mini Protein Gel (Thermo Fisher Scientific), and transferred to a PVDF membrane using an iBlot 2 gel transfer device (Thermo Fisher Scientific). After transfer, the membrane was immunoblotted with an anti-β Catenin antibody (Cell Signaling Technology, Danvers, MA, USA) using the iBind™ western device according to the manufacturer's protocol (Thermo Fisher Scientific). Subsequently, immunoreactive bands were visualized using an ECL solution (Thermo Fisher Scientific), and imaged by iBright™ CL1500 Imaging System (Thermo Fisher Scientific). Each Immunoreactive band was then quantified using Image J software (National Institutes of Health). Anti-β-actin antibody (Cell Signaling Technology) was used as an internal standard.

Measurement of hair growth factors and superoxide dismutase in mouse sera

After scarifying the mice, each serum sample were obtained, and the levels of mouse vascular endothelial growth factor (VEGF; Abcam, Cambridge, UK), mouse insulin-like growth factor-1 (IGF-1; Abcam) and mouse superoxide dismutase (SOD; MyBioSource, San Diego, CA, USA) were measured using sandwich enzyme-linked immunosorbent assay (ELISA) kits according to the manufacturer's protocols.

Flow cytometry analyses

Single-cell suspensions were prepared from vibrissa hair bulge from the back skin of experimental mice, according to a previously established method (Takeo et al., 2021). Cells were then resuspended in PBS containing 0.5% BSA, and stained

with FITC anti-mouse CD34 antibody (Thermo Fisher Scientific) and PE anti-mouse CD49f antibody (Thermo Fisher Scientific) for 15 min at 4℃. After staining, cells were analyzed by flow cytometry using BD FACSLyric™ (BD Biosciences, Mountain View, CA, USA) with BD FlowJo™ software (BD Biosciences).

Statistical analyses

All experimental data were presented as the mean±SD or mean±SEM. Statistical analysis was performed by two-tailed, unpaired Student's t-test for comparison between two independent variables, using Prism software (GraphPad Software, La Jolla, CA, USA).

Results and Discussion

LB-P9 increases hair cell proliferation and enhances the expression of vascular endothelial growth factor and fibroblast growth factor 7 by hair cells

The hFDPCs located at the dermal papilla of hair follicles are specialized mesenchymal cells that regulate the hair cycle and hair follicle formation (Matsuzaki and Yoshizato, 1998) while hGMCs are a major source of hair elongation and keratinization (Cribier et al., 2004). As an initial step to investigate the effect of LB-P9 on hair regeneration, we prepared LB-P9 CM, and treated with hGMCs and hFDPCs to test whether the treatment of LB-P9 CM affected the growth of hFDPCs or hGMCs. After the treatment of LB-P9 CM, the proliferation of hFDPCs was significantly increased in a dose-dependent manner. The treatment of 0.5 % LB-P9 also significantly increased the growth of hGMCs (Fig. 1A).

Next, we examined whether co-culture with LB-P9 stimulates hair growth factor production by hGMCs. Among hair growth factors, we measured the production of VEGF and fibroblast growth factor 7 (FGF-7) because these two cytokines are now considered to be key factors that accelerate hair regrowth after depilation (Guo et al., 1996; Madaan et al., 2018). In particular, VEGF enhances perifollicular vascularization, which leads to the increased size of vibrissa hair follicles and hair shafts (Yano et al., 2001), while FGF-7 which expresses the hair growth cycle is the major keratinocyte growth factor (Rosenquist and Martin, 1996). The results clearly indicated that co-culture with LB-P9 enhanced both VEGF and FGF-7 expressions by hGMCs more than two-fold (Fig. 1B). Taken together, the combined results demonstrate that LB-P9 might secrete soluble factors that facilitate hair cell growth and enhance the expression of VEGF and FGF-7 by hair cells through direct interaction. Similar to our observation, previous study reported that Minoxidil enhances the expression of VEGF in human hFDPCs (Lachgar et al., 1998).

Consumption of LB-P9 facilitates hair regeneration in animal model

Since we observed a stimulatory effect of LB-P9 on hair cell growth and the production of hair growth factors, we further determined whether LB-P9 consumption could facilitate hair regeneration using a time-synchronized depilation model. The time-synchronized depilation model is widely used to synchronize the hair cycle to monitor the hair regeneration rate to examine the hair growth stimulatory role of several reagents (Porter, 2003). For *in vivo* study, we orally administered a low dose of LB-P9 (4×10^7 CFU) or a high dose of LB-P9 (4×10^8 CFU) each day for four weeks after synchronizing the hair cycle. As a control, vehicle (PBS) was orally given to mice each day for four weeks.

As shown in Fig. 2A, visual analyses of the hair regrowth in experimental mice revealed that the oral administration of LB-P9 accelerated murine hair regrowth in a dose-dependent manner. Both the low dose and high dose-treated groups showed

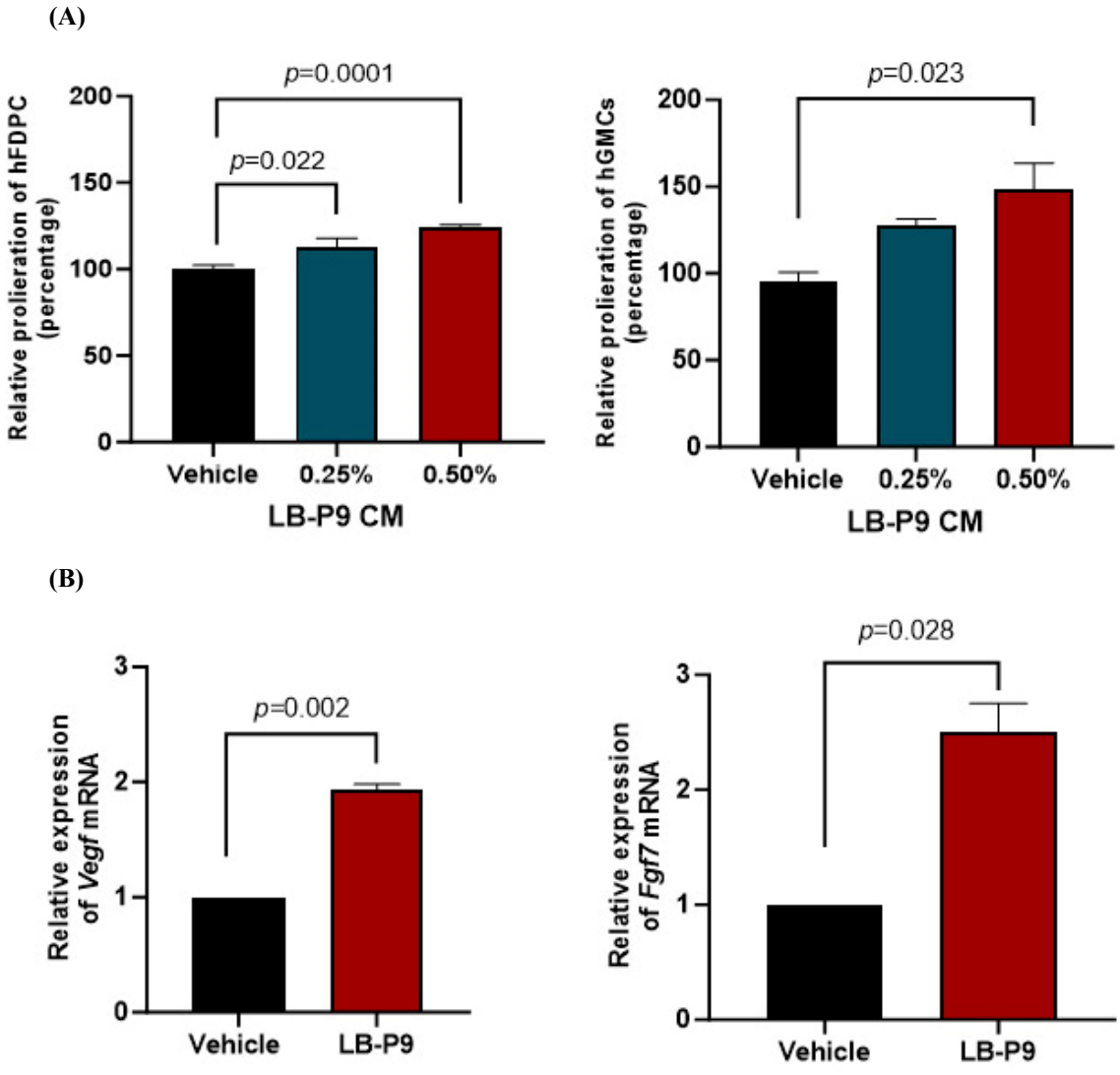

Fig. 1. LB-P9 facilitates hair cell proliferations and increases the expression of VEGF and FGF-7 by hair cells. (A) Both hFDPCs (1×10^4 cells/well) and hGMCs (1×10^4 cells/well) were cultured with 0.25% or 0.5% of LB-P9 CM at 96-well plate for 24 h. After culture, the relative proliferation ratio was measured using colorimetric assays (n=3). Vehicle, PBS treatment. Percentage indicated the concentration of LB-P9 CM in culture media. (B) The hGMCs (2×10^5 cells/well) were cultured with LB-P9 (2×10^6 CFU/well) at 6-well plate for 24 h. After culture, qRT-PCR analyses were performed to determine the relative expression levels of *Vegf* and *Fgf7* in hGMCs (n=3). Vehicle, PBS treatment; LB-P9, LB-P9 treatment. All results are shown as the mean±SD. Significant differences compared with the control group are indicated as "p=number". hFDPC, hair follicle dermal papilla cell; hGMC, hair germinal matrix cell; VEGF, vascular endothelial growth factor; FGF-7, fibroblast growth factor 7; CM, conditioned medium; PBS, phosphate-buffered saline; CFU, colony forming unit; qRT-PCR, quantitative reverse-transcriptase real-time polymerase chain reaction.

accelerated hair regrowth at day 12 until day 26 after the uptake of LB-P9, compared to that of the vehicle-treated group (Fig. 2B). After four-week treatment of LB-P9, the low dose-treated group failed to show a statistically significant hair regrowth rate higher than that of the vehicle-treated group (Fig. 2C). However, the high dose-treated group exhibited a significant increase of hair regrowth rate compared to that of the vehicle-treated group after the four-week treatment of LB-P9 (Fig. 2C).

Next, we determined whether the uptake of LB-P9 affects hair keratinization in mice. After scarifying mice, hairs were obtained from randomly selected animals from each different treatment group, and the hair thickness or hair cuticle shape measured by scanning electron microscopy. As shown in Fig. 2D, the average diameters of hairs from the LB-P9-treated

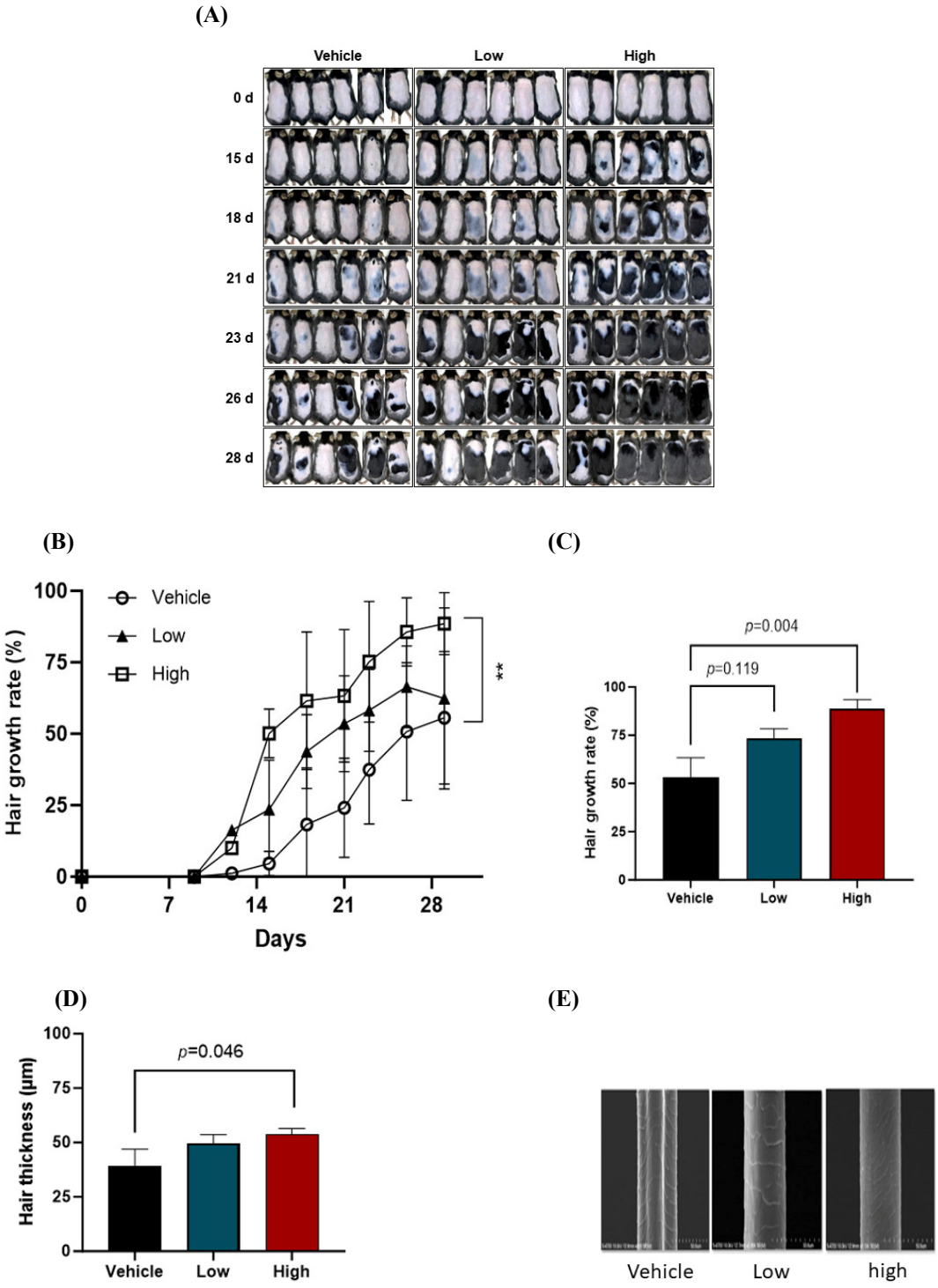

Fig. 2. Consumption of LB-P9 promotes hair regeneration in mice. Each group of C57BL/6 mice with telogen phase hair received a vehicle (PBS), low dose of LB-P9 (4×10^7 CFU in 200 μL of PBS), or high dose of LB-P9 (4×10^8 CFU in 200 μL of PBS) every day for 4 weeks (n=6 per group). (A) Visual analyses of hair regeneration from each group of mice for 4 weeks. "d" means days after administration of LB-P9. (B) Relative hair growth rate of each group of mice for 4 weeks during daily feeding of LB-P9. Hair growth rate (%)=regrown area/total shaved area. (C) Relative hair growth rate of each group of mice at 28 days after daily feeding of LB-P9. Hair growth rate (%)=regrown area/total shaved area. (D) Hair thickness of each group of mice at 28 days after daily feeding of LB-P9. (E) Representative scanning electron microscopy images (900× magnification) of the hair cuticle shapes of each group of mice at 28 days after daily feeding LB-P9. Vehicle, PBS administration; Low, low dose of LB-P9 (4×10^7 CFU) administration; high, high dose of LB-P9 (4×10^8 CFU) administration. Data are presented as the mean±SEM. Significant differences compared with the control group are indicated as "p=number". PBS, phosphate-buffered saline; CFU, colony forming unit.

groups were 49.546 μm (low dose) and 53.863 μm (high dose), respectively, whereas the average diameter of hairs from the vehicle-treated group was 39.283 μm. In particular, the average diameters of hairs from the high dose-treated groups were significantly greater than that of the vehicle-treated group (Fig. 2D). The hair cuticles protect the integrity of hair structure by wrapping around the hair cortex of hair fiber (Breakspear et al., 2022). Therefore, the shape of healthy hair cuticles maintains a dense overlay of each cuticle without cracks or holes (Kaliyadan et al., 2016). The scanning electron microscopy analyses indicated that the hair cuticle shape of the high dose-treated group had the densest overlay, without any cracks (Fig. 2E). Overall, these observations indicate that in the mouse model, the consumption of LB-P9 accelerates hair regeneration.

Consumption of LB-P9 systemically increases hair growth factor production and activates Wnt/β-catenin pathway in skin tissues

To define the molecular mechanism of how the consumption of LB-P9 improves hair regeneration, we first examined longitudinal and transverse sections of dorsal skin tissues from the experimental mice after H&E staining. Compared with the vehicle-treated group, the LB-P9 administrated group displayed increased number, length, and diameter of hair follicles in a dose-dependent manner (Figs. 3A and B). We also observed that the LB-P9-administered group showed an increased thickness of epidermis, compared to that of the vehicle-treated mice (Fig. 3C).

Wnt/β-catenin activation in hair follicles leads to hair growth by initiating anagen phase induction during the hair cycle progress (Kishimoto et al., 2000). In fact, several studies have shown that the loss of β-catenin in hair follicle stem cells (hFSCs) blocked hair regeneration, while the treatment of Wnt3a, one of the Wnt ligands, enhances the proliferation of hFSCs, and inhibits the apoptotic death of hFSCs (Jin et al., 2021; Kishimoto et al., 2000). To investigate the effect of LB-P9 on the Wnt/β-catenin pathway, we examined the β-catenin levels in the dorsal skin tissues from experimental mice. The results from immunoblot analyses indicated that the levels of β-catenin expression in skin tissues from high dose-treated mice were significantly increased, compared to the control groups (Fig. 3D). Supporting this observation, the number of hFSCs ($CD34^{+}CD49f^{+}$ cells) were significantly increased in the dorsal skin tissues of high dose-treated mice, compared to that of the vehicle-treated mice (Fig. 3E).

Previous observations demonstrated that IGF-1 triggers Wnt/β-catenin signaling, which induces the expression of VEGF, one of the important hair growth factors (Desbois-Mouthon et al., 2001; Goodwin and D'Amore, 2002). Interestingly, IGF-1 also serves as an important hair growth factor that affects hair cycle transition and the differentiation of hFSCs (Trüeb, 2018). Indeed, patients with Laron syndrome caused by the defect of IGF-1 signaling often exhibit defect of hair growth (Trüeb, 2018). Also, several previous reports indicated that accumulated oxidative stress in skin tissues might cause hair losses due to an aggravation of inflammatory responses around hair follicles (Ma et al., 2023). Therefore, we measured the levels of hair growth hormones such as IGF-1 and VEGF, and SOD in the sera of experimental mice by ELISAs. Results clearly indicated that the levels of serum IGF-1 and VEGF in the high dose-treated group were significantly increased, compared to the vehicle-treated group (Figs. 4A and B). In addition, the levels of serum SOD were significantly elevated in both low and high dose-treated groups compared to that of the vehicle-treated group (Fig. 4C). Taken together, the combined results demonstrate that the oral administration of LB-P9 might trigger the production of IGF-1 and VEGF that promote hair regeneration by the activation of Wnt/β-catenin pathway in skin tissues.

Among probiotics isolated from Kimchi, LB-P9 was originally selected based on a strong stimulatory effect on VEGF and FGF-7 productions by hGMCs. In our molecular model based on the combined results, LB-P9 administration systemically increases the production of hair growth factors such as IGF-1, FGF-7, and VEGF. Then, IGF-1 might activate Wnt/β-catenin

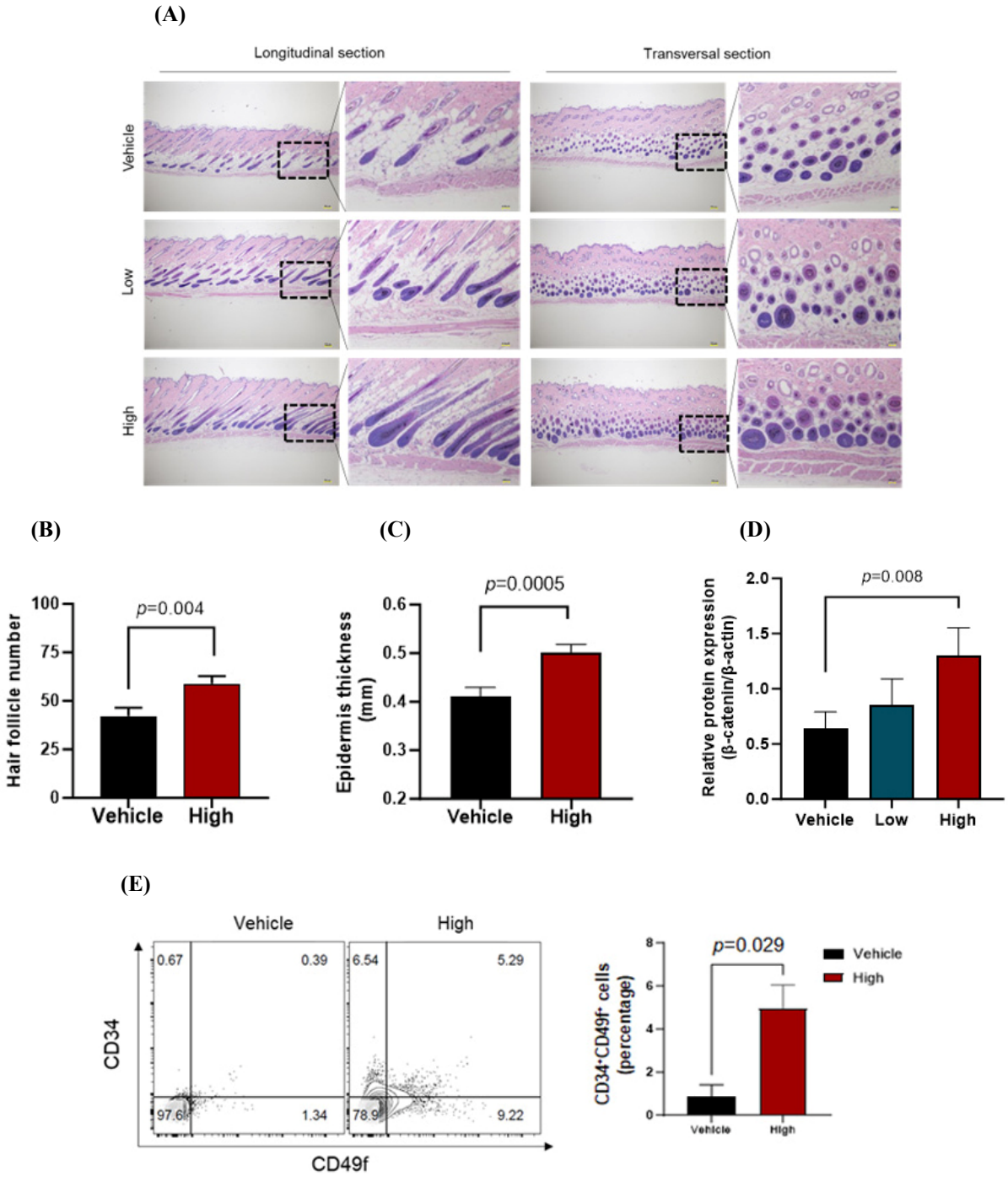

Fig. 3. Oral administration of LB-P9 enhances hair follicle formation by the activation of Wnt/β-catenin pathway and the increased frequency of hFSCs in skin tissues. (A–C) The architecture of skin dorsal tissues from each group of mice at 28 days after daily feeding of LB-P9 was examined by H&E staining (n=6). (A) Representative images of H&E staining results (40× magnification) in the longitudinal or transverse section of skin dorsal tissues from each group of mice. Inset shows enlarged images of hair follicles (200× magnification). Scale bar=100 μm. (B) Number of follicles and (C) thickness of dermis were measured in randomly selected pixel images (1.0×1.0 mm^2) of H&E staining tissues from each group of mice. (D) Relative expression of β-catenin in skin dorsal tissues from each group of mice examined by Western blot analyses (n=6). (E) Flow cytometry analyses of hFSCs ($CD34^+CD49f^+$ cells) in dorsal skin tissues from each group of mice (n=3) Representative image of flow cytometry analyses (left panel) and absolute cell number of hFSCs (right panel) in the skin dorsal tissues from each group of mice. Vehicle, PBS administration; Low, low dose of LB-P9 (4×10^7 CFU) administration; high, high dose of LB-P9 (4×10^8 CFU) administration. Data are presented as the mean±SEM. Significant differences compared with the control group are indicated as "p=number". hFSC, hair follicle stem cell; H&E, hematoxylin and eosin; PBS, phosphate-buffered saline; CFU, colony forming unit.

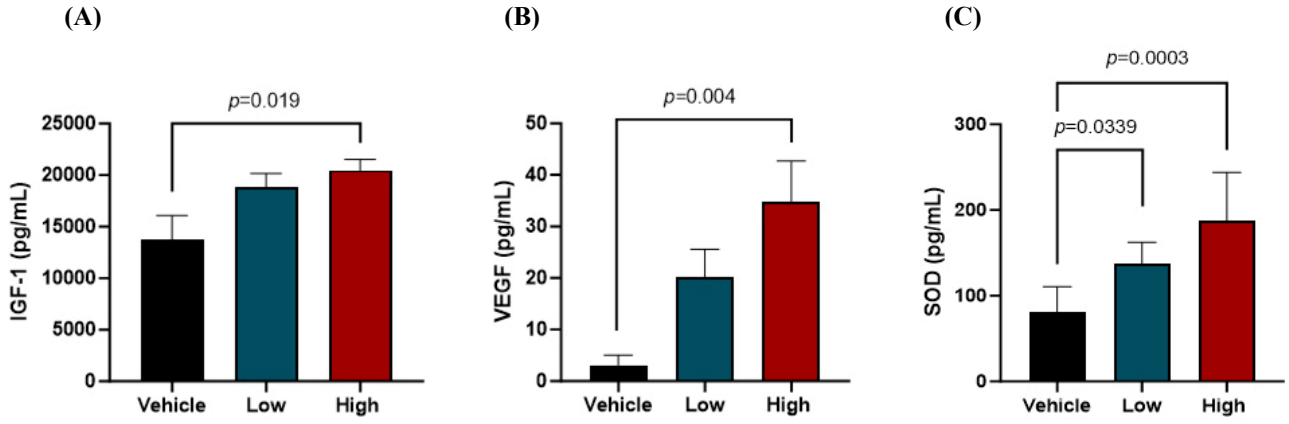

Fig. 4. Oral administration of LB-P9 systemically enhances production of hair growth factors and antioxidant enzyme. Mice of each group were sacrificed at 28 days after daily feeding LB-P9, and serum sample was prepared from each mouse. Subsequently, sandwich ELISAs were performed to measure the serum levels of (A) IGF−1, (B) VEGF, and (C) SOD (n=6). Vehicle, PBS administration; Low, low dose of LB-P9 (4×10^7 CFU) administration; high, high dose of LB-P9 (4×10^8 CFU) administration. Data are presented as the mean±SEM. Significant differences compared with the control group are indicated as "p=number". IGF-1, insulin-like growth factor-1; VEGF, vascular endothelial growth factor; SOD, superoxide dismutase; ELISA, enzyme-linked immunosorbent assay; PBS, phosphate-buffered saline; CFU, colony forming unit.

pathway, and IGF-1, FGF-7, or VEGF directly facilitates dermal papilla growth in skin tissues. Activation of the Wnt/β-catenin pathway further enhances hFSC or hair cell growth in skin tissues. The results of this study may provide additional evidence to support the idea that the consumption of probiotics enhances hair growth.

Further study is required to dissect the fine molecular mechanism of how the interaction between LB-P9 and intestinal epithelial cells induces hair growth factor production. Especially, the identification of soluble factors secreted by LB-P9 which facilitate the growth of hGMCs is required to understand a precise signaling pathway of hGMC proliferation by LB-P9. Also, the examination on changes in the composition of gut microbiota after LB-P9 administration strengthens the theory about "gut-brain-skin axis'.

Conclusion

Our data suggest that hair regeneration might be facilitated by the consumption of a specific strain of probiotics by enhancing dermal papilla growth via the systemic augmentation of hair growth factor production, resulting the activation of Wnt/β–catenin pathway in skin tissues.

Conflicts of Interest

Mikyung Song, Jaeseok Shim, and Kyoungsub Song are currently employed by LISCure Biosciences Inc., Korea.

Author Contributions

Conceptualization: Shim J, Song K. Data curation: Song M, Shim J, Song K. Formal analysis: Song M, Song K. Methodology: Song M, Shim J, Song K. Software: Song M, Song K. Validation: Song M, Shim J, Song K. Investigation:

Song M, Shim J, Song K. Writing - original draft: Song M, Song K. Writing - review & editing: Song M, Shim J, Song K.

Ethics Approval

The protocol of animal study was approved by the Institutional Animal Care and Use Committee of CentralBio Co., Ltd. (protocol number: CBIACUC 22-0478EF).

References

Arck P, Handjiski B, Hagen E, Pincus M, Bruenahl C, Bienenstock J, Paus R. 2010. Is there a 'gut–brain–skin axis'? Exp Dermatol 19:401-405.

Bajoria PS, Dave PA, Rohit RK, Tibrewal C, Modi NS, Gandhi SK, Patel P. 2023. Comparing current therapeutic modalities of androgenic alopecia: A literature review of clinical trials. Cureus 15:e42768.

Belkaid Y, Hand TW. 2014. Role of the microbiota in immunity and inflammation. Cell 157:121-141.

Breakspear S, Ivanov DA, Noecker B, Popescu C, Rosenthal M. 2022. Cuticle: Designed by nature for the sake of the hair. Int J Cosmet Sci 44:343-362.

Cribier B, Peltre B, Grosshans E, Langbein L, Schweizer J. 2004. On the regulation of hair keratin expression: Lessons from studies in pilomatricomas. J Invest Dermatol 122:1078-1083.

Desbois-Mouthon C, Cadoret A, Blivet-Van Eggelpoël MJ, Bertrand F, Cherqui G, Perret C, Capeau J. 2001. Insulin and IGF-1 stimulate the *β*-catenin pathway through two signalling cascades involving GSK-3*β* inhibition and Ras activation. Oncogene 20:252-259.

Dumas A, Bernard L, Poquet Y, Lugo-Villarino G, Neyrolles O. 2018. The role of the lung microbiota and the gut–lung axis in respiratory infectious diseases. Cell Microbiol 20:e12966.

Goodwin AM, D'Amore PA. 2002. Wnt signaling in the vasculature. Angiogenesis 5:1-9.

Guo L, Degenstein L, Fuchs E. 1996. Keratinocyte growth factor is required for hair development but not for wound healing. Genes Dev 10:165-175.

Jin H, Zou Z, Chang H, Shen Q, Liu L, Xing D. 2021. Photobiomodulation therapy for hair regeneration: A synergetic activation of *β*-CATENIN in hair follicle stem cells by ROS and paracrine WNTs. Stem Cell Rep 16:1568-1583.

Kaliyadan F, Gosai BB, Al Melhim WN, Feroze K, Qureshi HA, Ibrahim S, Kuruvilla J. 2016. Scanning electron microscopy study of hair shaft damage secondary to cosmetic treatments of the hair. Int J Trichol 8:94-98.

Kishimoto J, Burgeson RE, Morgan BA. 2000. Wnt signaling maintains the hair-inducing activity of the dermal papilla. Genes Dev 14:1181-1185.

Lachgar S, Charveron M, Gall Y, Bonafe JL. 1998. Minoxidil upregulates the expression of vascular endothelial growth factor in human hair dermal papilla cells. Br J Dermatol 138:407-411.

Lee J, Yang W, Hostetler A, Schultz N, Suckow MA, Stewart KL, Kim DD, Kim HS. 2016. Characterization of the anti-inflammatory *Lactobacillus reuteri* BM36301 and its probiotic benefits on aged mice. BMC Microbiol 16:69.

Ma Y, Sun Z, Li YM, Xu H. 2023. Oxidative stress and alopecia areata. Front Med 10:1181572.

Madaan A, Verma R, Singh AT, Jaggi M. 2018. Review of hair follicle dermal papilla cells as *in vitro* screening model for hair growth. Int J Cosmet Sci 40:429-450.

Matsuzaki T, Yoshizato K. 1998. Role of hair papilla cells on induction and regeneration processes of hair follicles. Wound

Repair Regen 6:524-530.

Nam W, Kim H, Bae C, Kim J, Nam B, Kim J, Park S, Lee J, Sim J. 2021. *Lactobacillus paracasei* HY7015 promotes hair growth in a telogenic mouse model. J Med Food 24:741-748.

Nestor MS, Ablon G, Gade A, Han H, Fischer DL. 2021. Treatment options for androgenetic alopecia: Efficacy, side effects, compliance, financial considerations, and ethics. J Cosmet Dermatol 20:3759-3781.

Park DW, Lee HS, Shim MS, Yum KJ, Seo JT. 2020. Do Kimchi and *Cheonggukjang* probiotics as a functional food improve androgenetic alopecia? A clinical pilot study. World J Mens Health 38:95-102.

Porter RM. 2003. Mouse models for human hair loss disorders. J Anat 202:125-131.

Powell N, Walker MM, Talley NJ. 2017. The mucosal immune system: Master regulator of bidirectional gut–brain communications. Nat Rev Gastroenterol Hepatol 14:143-159.

Rosenquist TA, Martin GR. 1996. Fibroblast growth factor signalling in the hair growth cycle: Expression of the fibroblast growth factor receptor and ligand genes in the murine hair follicle. Dev Dyn 205:379-386.

Takeo M, Asakawa K, Toyoshima K, Ogawa M, Tong J, Irié T, Yanagisawa M, Sato A, Tsuji T. 2021. Expansion and characterization of epithelial stem cells with potential for cyclical hair regeneration. Sci Rep 11:1173.

Tamashunas NL, Bergfeld WF. 2021. Male and female pattern hair loss: Treatable and worth treating. Cleve Clin J Med 88:173-182.

Tripathi A, Debelius J, Brenner DA, Karin M, Loomba R, Schnabl B, Knight R. 2018. The gut–liver axis and the intersection with the microbiome. Nat Rev Gastroenterol Hepatol 15:397-411.

Trüeb RM. 2018. Further clinical evidence for the effect of IGF-1 on hair growth and alopecia. Skin Appendage Disord 4:90-95.

Yano K, Brown LF, Detmar M. 2001. Control of hair growth and follicle size by VEGF-mediated angiogenesis. J Clin Invest 107:409-417.